SCRUTINIZATION OF KRYLOV SUBSPACE METHOD FOR THE SOLUTION OF ELECTRIC DOUBLE LAYER EFFECT ON THERMAL LINE CONTACT ELASTO-HYDRODYNAMIC LUBRICATION PROBLEM

Mahesh Kumar N. – Vishwanath B. Awati* – Parashuram M. Obannavar

Department of Mathematics, Rani Channamma University, Belagavi-591156, Karnataka, India.

ARTICLE INFO

***Article history*:**
Received: 05.01.2024.
Received in revised form: 02.12.2024.
Accepted: 13.12.2024.

Keywords:
Thermal EHL;
Apparent viscosity
EDL
Newton-GMRES
Daubechies D6 wavelet
pre-conditioner

DOI: https://doi.org/10.30765/er.2432

Abstract:

The paper presents, the numerical investigation of electrical double layer (EDL) effect on thermal elasto-hydrodynamic lubrication (EHL) line contact problem. The precise mathematical model consists of modified Reynolds, film thickness, load balance, and energy equations along with appropriate boundary conditions. The numerical computation of the problem involves apparent viscosity along with viscosity-pressure-temperature and density-pressure-temperature relations. The second order finite difference approximations are used to discretize the governing mathematical equations. The resulting systems of non-linear algebraic equations are solved using Newton-generalized minimum residual (GMRES) method with Daubechies D6 wavelet as pre-conditioner. The temperature grown freely in EHL contact area, the influence of temperature rise on EDL effect is studied in detail.The results illustrates that, film thickness increases with increase in EDL effect. The minimum film thickness for isothermal case is larger as compared to thermal film thickness and temperature escalation in contacting region reduces the film thickness. The EDL effect enhances fluid film thickness, while temperature rise in the contact area reducesminimum film thickness. Comparison between isothermal and the thermal results are presented in the form of figures and tables.

1 Introduction

Advances in science, technology and materials research have led to the use of ceramic materials in the construction of many machine components such as cams, gears, etc. These material surfaces are less rough compared to other material surfaces. The separation between two ceramic materials requires a thinner film thickness, resulting in a thinner lubricating film thickness as the effect of the electrical double layer is greater; this phenomenon is known as thin film lubrication (TFL). The decades of studies show that TFL reduces the friction coefficients of ceramic materials by a thin water film of 30-40 nm thickness [1], as water is readily available and environmentally friendly by nature. The rheological properties of the lubricant in TFL differ from those of thick film lubrication. All these aspects raise attention and help to understand the phenomenon of electrokinetic effects induced by EDL.

Prieve and Bike [2] deliberated the electro-kinetic repulsion between two charged bodies undergoing the sliding motion. The study of lubrication analysis for bodies bearing thin double layer while considering squeeze and sliding motion was studied by Bike and Prieve [3]. Luo et al. [4]experimentally deliberated the difference between EHL and TFL. Zhang and Umehara [5] analyzed the hydrodynamic lubrication problem lubricated with water and presented the modified Reynolds equation. The effect of EDL on flow characteristics of dilute aqueous solutions in small micro-channels was discussed by Li [6]. Ren et al.

*Corresponding author
E-mail address: awati.vb@rcub.ac.in

[7]considered the electro-viscous effect on fluid flow in micro-channels. The magnitude of additional flow resistance caused by electro-kinetic effect in micro-channels was discussed by Ren et al. [8]. Huang et al. [9], and Wong et al. [10], numerically studied the consequences of hydrodynamic and Elasto-hydrodynamic lubrication (EHL) problems. Li [11] discussed the surface roughness on EHL with thin EDL for sliding of one charged body past another in an electrolyte solution. The effect of EDL on TFL was demonstrated experimentally by Bai et al.[12], further derived a complete mathematical model to understand the electro-viscous influence caused by EDL on friction surfaces. A series of experimental and theoretical investigations are accomplished by Shaoxian and Ping [13], Wang et al. [14], and Bai [15] to realize the outcomes of EDL on lubricating film. The small dimension effect like EDL is mainly depends on the size of film thickness and lubricant properties were noticed by Wen [16]. But the practical problem is more complex, even though a rigid surface undergoes elastic deformation when they are subjected to high pressure. As compared to hydrodynamic withEHL theories, it predicts that, larger film thickness under the same operating conditions.

Chen et al. [17] explored the EHL line contact problem by considering EDL effect and noticed that, EDL has significant impact on film thickness. Awati et al. [18] deliberated the effect of EDL on EHL line contact problem with surface roughness and predict that, EDL has less impact on pressure and significant impact on film thickness. In most of the frictional work heat is produced due to scraping of surfaces. Because of this phenomenon heat is generated within the contact region that affects the performance of the machine components. Thus, it is important to consider the effect of temperature while analyzing EHL problems. The consideration of temperature effects in EHL analysis dates back to 1961. in 1961, the Newton-Raphson method for predicting temperature effects in EHL problems was studied by Cheng and Sternlicht [19].

The formula for calculating the minimum layer thickness was presented by Ghosh and Hamrock [20]. The Newton-Raphson method is used by Sadeghi and Sui [21] to study the behaviour of temperature in the EHL line contact problem. Salehizadeh and Saka [22] analyzed the temperature effects in EHL problem by considering non-Newtonian fluid with rolling/sliding conditions. Many researchers examine the effects of temperature on EHL problem with different physical models, techniques and lubricants [23], [24]. Liu and Yang [25] deliberated the thermal effects on finite EHL line contact problem. Yang et al. [26] studied the starvation, thermal and non-Newtonian behavior of EHL line contact problem. The numerical solution of thermal EHL point contact problem was studied by Habachi et al. [27]with Newtonian as well as non-Newtonian fluids. Carli et al. [28] scrutinize the thermal EHL point contact with rolling/sliding condition through numerically as well as experimentally. The effect of temperature on EDL and EHL point contact problem was discussed numerically by Zuo et al. [29]. The fatigue life of machine components in point contact EHL problem was explored by Yan et al. [30]. The performance of thermal EHL line contact problem under zero entertainment velocity with Newtonian and Ree-Eyring fluid models was examined by Zhang et al. [31].

The impact of thermal conductivity of contacting surfaces on traction in rolling/sliding EHL problem was numerically discussed by Liu et al. [32]. So far EHL studies focused on a velocity slip at the solid-lubricant interface. But the fluid film thickness mainly depends on the boundary slip, thermal slip at the solid-lubricant interface was revealed by Meng et al. [33]. Ono [34] deliberated the modified Reynolds equation for the study of thin film lubrication with high viscosity, to analyze the mechanism of high load capacity and super-low friction coefficient in micro-texture lubrication.Awati et al. [35] studied the numerical solution of thermal EHL line contact problem with bio-based oil as lubricant. Tosic et al. [36] considered the non-Newtonian rheology and thermal effects on slender EHL contacts via both experimental and numerical study. The fully coupled mixed finite line contact EHL problem was solved by Fang et al. [37] using finite element method. Further the investigation reveals that, 5% higher accuracy and 50% greater efficiency as compared to weakly coupled one. To solve the EHL problem as effectively as possible, there are new ideas for artificial neural networks (ANN). Yu et al [38], among others, used a backpropagation neural network (BPNN) to solve the EHL problem, which accurately predicts the oil pressure and film thickness.

Thermal EHL scrutinizes the non-wetting/wetting contact under a high slide to roll ratio to realize interplay of boundary slip and heat was debated by Zhao and Wong [39]. Hjelm and Wahlstrom [40] premeditated the influence of manufacturing error tolerance on thermal EHL behavior of gears.

Most of the EHL line contact problems were solved numerically through Newton-Raphson technique. The demerits of Newton-Raphson method is that, the computational cost of the method is $O(n^3)$, n is the number of calculation points in the calculation domain, as n increases the condition number of Jacobian matrix also increases. The elastic deformation term in Jacobian matrix, which is a $n \times n$ matrix and finding its inverse requires $O(n^3)$ operations. For high load and speed, Jacobian matrix becomes dense, sparse and singular. This difficultly can be evaded by using much lower complexity schemes for the solution of problem. One typical procedure is to apply FAS method having lower complexity i.e $O(n \log n)$ it is one of the most efficient method as compared to Newton-Raphson method. In this method, the spatial domain is divided into two regions and solutions of these regions are obtained by using Gauss-Seidel and Jacobi di-pole iteration methods. The Newton-GMRES method with Daubechies D6 wavelet as pre-conditioner is used, to reduce the condition number of Jacobian matrix which in turn reduces the number of iterations for convergence as compared to other numerical methods.

1.1 Krylov subspace method (KSM)

Consider a system of linear algebraic equations

$$Ax = b \tag{1}$$

where, A be a dense, non-symmetric matrix and Eqn. (1) is solved by using Krylov subspace iterative method [41] viz. Generalized Minimum Residual(GMRES) method. KSM was introduced by Hestenes and Stiefel [42] for the solution of linear system of large sparse algebraic equations as direct method. Reid[43] re-introduced them as iterative methods and Golub and Leary [44] developed these methods. Greenbaum [45]presented the salient features of these KSM methods. Saad and Schultz [46]depicted the GMRES method from the generalization of MINRES algorithm i.e. extension of Arnoldi process and researchers like, Saad and Vorst [47], Roland et al. [48], Simoncini and Szyld [49] have extended the KSM. However, the convergence of GMRES method is too slow when the grid size n increases. Thus, the convergence of GMRES method can be accelerated for the matrix A is first preconditioned. Hence, pre-conditioner with GMRES method is used to solve large system of equations. Let us construct the sparse matrix P using discrete wavelet transforms and approximate matrix A is right preconditioned, then Eqn. (1) becomes

$$AP^{-1}y = b, \qquad \text{where } y = Px,$$

And P is a noble approximation to A, then it requires less number of iterations to achieve the convergence with error tolerance. To approximate a full matrix A, we first consider a Discrete Wavelet Transform (DWT) constitute with Daubechies D6 wavelet, with Permutation as proposed by Chen [50]. In this paper all the results are accomplished by using Daubechies D6 wavelet [51] transform.

Let m be the order of compactly supported wavelets with m low pass filter coefficients $c_0, c_1, c_2, ..., c_{m-1}$ and $\frac{m}{2}$ vanishing movements. The coefficients $d_0, d_1, ..., d_{m-1}$ are derived from c_i by the relation $d_i = (-1)^i c_{m-1-i}$. Let us consider $n = 2$ and $2^{\hat{r}} < m$ and $2^{\hat{r}+1} \geq m$, where ℓ is the resolution level in the Krylov subspace, and $\hat{r}$ is integer $0 < \hat{r} < \ell$. Indicate $s = s^{\ell}$ is a column vector in the matrix A at the wavelet level ℓ and f is a given function. The wavelet transform $W : s \to w$ (i.e. $w = Ws$) is implemented by well-known pyramidal algorithm. The standard pyramidal algorithm transforms the vector s^{ℓ} to $w = \left[\left(s^{\hat{r}}\right)^T \left(f^{\hat{r}}\right)^T \left(f^{\hat{r}+1}\right)^T ... \left(f^{\ell-1}\right)^T \right]^T$ in a level by level manner, where $s^{(v)}$ and $f^{(v)}$ are of length 2^v. The sum of all these lengths is 2^{ℓ} and $v = \ell - 1, ..., \hat{r} + 1$.

At the characteristic level v, $s^{(v)}$ and $f^{(v)}$ are the collections of scaling and wavelet coefficients respectively. In matrix form, w can be expressed as $w = P_{\hat{r}+1} W_{\hat{r}+1} P_{\hat{r}+2} W_{\hat{r}+2} ... P_{\ell-1} W_{\ell-1} P_{\ell} W_{\ell} = Ws^{\ell}$, where

$$P_v = \begin{pmatrix} \overline{P_v} & \\ & J_v \end{pmatrix}_{n \times n} \quad \text{and} \quad W_v = \begin{pmatrix} \overline{W_v} & \\ & J_v \end{pmatrix}_{n \times n},$$

$\overline{P}_\nu$, is a permutation matrix, $\overline{W}_\nu$ is an orthogonal (sparse) matrix of size $2^\nu = 2^\ell - k_\nu = n - k_\nu$, i.e. $\overline{P}_\nu = I(1,3,...,2^\nu - 1,2,4,...,2^\nu)$, J_ν is an identity matrix of size k_ν. Here $k_\ell = 0$ and $k_\nu = k_{\nu+1} + 2^\nu$ for $\nu = \ell - 1,...,\hat{r} + 1$

The one level transformation matrix $\overline{W}_\nu$ with Daubechies wavelet transform of order $m = 6$ with $m/2 = 3$ vanishing moments becomes

$$\overline{W} = \begin{pmatrix}
c_0 & c_1 & c_2 & c_3 & c_4 & c_5 & & & & & & \\
d_0 & d_1 & d_2 & d_3 & d_4 & d_5 & & & & & & \\
 & & c_0 & c_1 & c_2 & c_3 & c_4 & c_5 & & & & \\
 & & d_0 & d_1 & d_2 & d_3 & d_4 & d_5 & & & & \\
 & & & & \cdot & \cdot & \cdot & \cdot & \cdot & \cdot & & \\
 & & & & \cdot & \cdot & \cdot & \cdot & \cdot & \cdot & & \\
 & & & & & & & & & & & \\
 & & & & & & & & \cdot & \cdot & \cdot & \cdot \\
 & & & & & & & & \cdot & \cdot & \cdot & \cdot \\
c_4 & c_5 & & & & & & & c_0 & c_1 & c_2 & c_3 \\
d_4 & d_5 & & & & & & & d_0 & d_1 & d_2 & d_3 \\
c_2 & c_3 & c_4 & c_5 & & & & & & & c_0 & c_1 \\
d_2 & d_3 & d_4 & d_5 & & & & & & & d_0 & d_1
\end{pmatrix}_{n \times n}$$

where $\{c_i, d_i\}$ are the filtering coefficients known to be $c_0 = 0.33267$, $c_1 = 0.80689$, $c_2 = 0.45987$, $c_3 = -0.13501$, $c_4 = 0.08544$, $c_5 = 0.03522$ and $d_k = (-1)^k c_{m-1-k}$.

1.2 Discrete wavelet transformation with permutation (DWTPer)

Let the matrix A can be written in terms of DWTPer is expressed as $\hat{A} = \hat{W} A \hat{W}^{\mathrm{T}}$, where $\hat{W} = PW$ and permutation matrix $P = P_L^{\mathrm{T}} P_{L-1}^{\mathrm{T}} ... P_{r+2}^{\mathrm{T}} P_{r+1}^{\mathrm{T}}$. In this instance, permutation D6 discrete wavelet transformation is utilized to Jacobian matrix with thresholding i.e., setting the elements below some numerical value to zero. A simple pre-conditioner for such a matrix would be a banded matrix it can be constructed by setting to zero for all entries of the matrix outside a chosen diagonal band [Ford et al. [52]]. The band matrices make a particularly good pre-conditioner as it may be stored efficiently and there are subroutines available for manipulating them at low cost. The application of DWT on sparse and dense matrix with D6 wavelet generates more non-zero elements analogize to DWT with D4 wavelet coefficients. Hence the precision and convergence of this technique increases for DWT with D6 wavelet co-efficients.

The paper presents a numerical computation of EDL effect on thermal EHL line contact problem with water as lubricant. The precise mathematical model consist of modified Reynolds, film thickness, load balance and energy equations and these are solved simultaneously using Newton-GMRES method with Daubechies D6 wavelet as pre-conditioner. The physics of EHL is discussed for various operating parameters and the effect of EDL, temperature on film thickness and pressure profiles are illustrated in the form of figures and tables.

2 Governing Equations

Consider an electric double layer take place between the solid/liquid interfaces. The steady state thermal modified Reynolds equation[53] is given in dimensionless form as

$$\frac{\partial}{\partial X}\left(\varepsilon \frac{\partial P}{\partial X}\right) - \lambda\left(\frac{\partial(\hat{\rho}H)}{\partial X}\right) = 0\,, \tag{2}$$

where, $\varepsilon = \dfrac{\hat{\rho} H^3}{\eta_a^*}$, $\hat{\rho}$ and H denotes the dimensionless density and fluid film thickness respectively, P is the fluid film pressure and $\lambda = \dfrac{12U^* E' \hat{R}^3}{P_h b^3}$. The apparent viscosity η_a^* of the lubricant, for the present study it is expressed as[12],

$$\eta_a^* = \ddot{\eta} + \frac{3\ddot{\varepsilon}^2 \xi^2 \hat{R}^4}{4\pi^2 \kappa^2 b^8 \eta_0 \tilde{\lambda}} \frac{1}{H^4} \left[\frac{\left(\cosh \kappa \left(\dfrac{Hb^2}{\hat{R}} \right) - 1 \right)^2}{\sinh \kappa \left(\dfrac{Hb^2}{\hat{R}} \right)} - \sinh \kappa \left(\frac{Hb^2}{\hat{R}} \right) + \kappa \left(\frac{Hb^2}{\hat{R}} \right) \right]^2, \tag{3}$$

where, $\ddot{\varepsilon}$ is the absolute dielectric constant of the fluid, κ is the Debye reciprocal length, $\ddot{\eta}$ is the viscosity of lubricant, ξ is the zeta potential of EDL, $\tilde{\lambda}$ is the bulk electrical conductivity and the electro viscosity is expressed as

$$\eta_e = \frac{3\ddot{\varepsilon}^2 \xi^2 \hat{R}^4}{4\pi^2 \kappa^2 b^8 \eta_0 \tilde{\lambda}} \frac{1}{H^4} \left[\frac{\left(\cosh \kappa \left(\dfrac{Hb^2}{\hat{R}} \right) - 1 \right)^2}{\sinh \kappa \left(\dfrac{Hb^2}{\hat{R}} \right)} - \sinh \kappa \left(\frac{Hb^2}{\hat{R}} \right) + \kappa \left(\frac{Hb^2}{\hat{R}} \right) \right]^2, \tag{4}$$

H is the fluid film thickness. The fluid film thickness equation in dimensionless form is given by

$$H(X) = H_0 + \frac{X^2}{2} - \frac{2}{\pi E'} \int_{X_{in}}^{X_{out}} P(X') \ln(X - X') dX'. \tag{5}$$

where H_0 denotes the dimensionless offset film thickness.
The viscosity-pressure-temperature relation in dimensionless form as [54]

$$\ddot{\eta} = \exp\left\{ \left[\ln(\eta_0) + 9.67 \right] \left[-1 + (1 + 5.1 \times 10^{-9} P_h P)^{0.68} \right] - \gamma T_0 (\hat{T} - 1) \right\}, \tag{6}$$

where, γ is the temperature-viscosity coefficient. The density-pressure-temperature relation is expressed in non-dimensional form as [55]

$$\hat{\rho} = \left[1 + \left(\frac{0.6 \times 10^{-09} P P_h}{1 + 1.7 \times 10^{-09} P P_h} \right) \right] + D_0 T_0 \left(\hat{T} - 1 \right), \tag{7}$$

where $D_0 = -0.00065$. The relevant boundary conditions of Reynolds equations is given in dimensionless form as

$$P(X) = 0, \quad \text{at } X = X_{in}, \text{ and } \frac{dP}{dX} = 0, \text{ at } X = X_{out}. \tag{8}$$

The load balance equation in non-dimension form as

$$\int_{X_{in}}^{X_{out}} P(X) dX = \frac{\pi}{2}. \tag{9}$$

For the study of thermal EHL problem, the energy equation is elucidated to compute temperature in the contact region and dimensionless form of energy equation becomes

$$\frac{\partial^2 \hat{T}}{\partial Z^2} = F_1\left(\hat{\rho}U^*\frac{\partial \hat{T}}{\partial X}\right) - F_2\left(\frac{\hat{T}}{\hat{\rho}}\frac{\partial P}{\partial X}\right) - F_3\left(\eta_a^*\left(\frac{\partial U^*}{\partial Z}\right)^2\right) \tag{10}$$

where, $F_1 = \dfrac{\rho_0 C_p E' b^3}{K\eta_0 \hat{R}}$, $F_2 = \dfrac{E' P_h b^3}{K\eta_0 R \rho_0}$ and $F_3 = \dfrac{E'^2 \hat{R}^2}{K\eta_0 T_0}$. The boundary conditions for two interfaces are expressed in dimensionless form as

$$\hat{T}_{up1}(X) = \frac{K}{\sqrt{\pi\rho_1 C_1 K_1 U_1}} \int_{X_{in}}^{X_{out}} \left(\frac{\partial \hat{T}}{\partial Z}\right)_{Z=0} \frac{dX'}{\sqrt{X - X'}}, \tag{11}$$

$$\hat{T}_{dwn2}(X) = \frac{K}{\sqrt{\pi\rho_2 C_2 K_2 U_2}} \int_{X_{in}}^{X_{out}} \left(\frac{\partial \hat{T}}{\partial Z}\right)_{Z=H} \frac{dX'}{\sqrt{X - X'}}, \tag{12}$$

where, thermal conductivity of lubricant, steel and ceramic material (SiO_2) are denoted as K, K_1 *and* K_2 respectively. C_1 and C_2 are the specific heat of upper and lower surfaces respectively, ρ_1 and ρ_2 are the densities of upper and lower surfaces, U_1 and U_2 are the velocities respectively denotes the upper and lower surfaces, η_0 is the ambient viscosity of lubricant and non-dimensional parameters used in the present study is

$$\hat{\rho} = \frac{\rho}{\rho_0},\quad \eta_a^* = \frac{\eta_a}{\eta_0},\quad \ddot{\eta} = \frac{\eta}{\eta_0},\quad P = \frac{p}{P_h},\quad X = \frac{x}{b},\quad Z = \frac{z\hat{R}}{b^2},\quad \hat{T} = \frac{T}{T_0},\quad \mathrm{W} = \frac{w}{E'R},\quad U^* = \frac{\eta_0 u_s}{E'\hat{R}}\ . \tag{13}$$

2.1 Discretization of governing equations

In the present study, the interval of computation is considered as X_{in}*=-4 and* X_{out}*=1.4* with uniform 513 grid points. Finite difference technique of second order were used to discretize the governing equations,and discretization of Reynolds equation becomes

$$\frac{(\zeta_i + \zeta_{i+1})(P_{i+1} - P_i) - (\zeta_i + \zeta_{i-1})(P_i - P_{i-1})}{\Delta X^2} - \frac{H_i - H_{i-1}}{\Delta X} = 0, \tag{14}$$

where, $\Delta X = \dfrac{X_{out} - X_{in}}{N+1}$, $\zeta = \dfrac{\varepsilon}{\lambda}$, $\varepsilon = \dfrac{\hat{\rho}H^3}{\eta_a^*}$, $\lambda = \dfrac{12U^* E' R^3}{P_h b^3}$.

The boundary conditions in discretized form as

$$P(X_{in}) = 0 \text{ and } \frac{P(X_{out}) - P(X_{out-1})}{\Delta X}. \tag{15}$$

The film thickness equation can be discretized as

$$H_i = H_0 + \frac{X_i}{2} - \frac{1}{\pi}\sum_{j=1}^{N} K_{ij} P_j, \tag{16}$$

where K_{ij} is the kernel given by

$$K_{ij} = +\left(i - j + \frac{1}{2}\right)\Delta X\left[\ln\left(\left|i - j + \frac{1}{2}\right|\Delta X\right) - 1\right] - \left(i - j - \frac{1}{2}\right)\Delta X\left[\ln\left(\left|i - j - \frac{1}{2}\right|\Delta X\right) - 1\right]. \tag{17}$$

The discretization of load balance equation becomes

$$\Delta X \sum_{i=1}^{N} \frac{(P_i + P_{i+1})}{2} = \frac{\pi}{2}. \tag{18}$$

The non-dimensional energy equation can be expressed in discretized form as

$$F_1\left(\frac{\hat{T}_{i,kk} - \hat{T}_{i-1,kk}}{\Delta X}\right) + F_2 \frac{\hat{T}}{\hat{\rho}}\left(U^* \frac{P_{i,j} - P_{i-1,j}}{\Delta X}\right) + \left(\frac{\hat{T}_{i,kk+1} - 2\hat{T}_{i,kk} + \hat{T}_{i,kk-1}}{\Delta Z^2}\right) \tag{19}$$

$$+F_3 \eta_a^* \left(\frac{U^*_{i,kk+1} - U^*_{i,kk}}{\Delta Z}\right)^2 = 0,$$

where, *kk* indicates the node number in the film thickness direction.

2.2 Solution procedure

The leading mathematical equations are discretized by using finite difference approximations, the resulting system of non-linear equations were solved by using Krylov subspace method. We, first convert the non-linear system of equations into linear system of equations by Newton's method. To solve these linear system of equations $Ax = b$, many methods are available in the literature. But Krylov-subspace methods are more suitable and robust technique [56] to solve the large system of linear equations. Depending upon the properties of the matrix *A (*symmetry, positive definite, indefinite, asymmetric etc.,*)* different Krylov subspace methods are available [41], [47]in the literature. In this situation, resulting matrix *A* is a sparse and dense. GMRES method is more appropriate and robust to solve the system of linear equations. The pre-conditioner is used because the problem is highly non-linear in nature, the resulting matrix has large condition number, in order to reduce the condition number nearer to unity the problem is well behaved and it is easy to determinethe required solution in reduced number of iterations.

First we obtain the isothermal pressure and film thickness values by utilizing the preconditioned Newton-GMRES method. The energy equation is solved using finite difference method with Gauss-Seidel iteration method and utilizing the attained pressure and film-thickness. The resulting temperature, pressure, film thickness are used in the calculation of isothermal pressure and film thickness recursively. The process is repeated until the converged solution is obtained.

3 Results and discussion

The present work is to investigate EDL effect on film thickness and temperature is explored over a 513 uniform grid points on a computational domain $-4 \le X \le 1.4$. The Newton-GMRES technique with Daubechies D6 wavelet as pre-conditioner is employed to solve the nonlinear system of coupled equations. The effect of EDL on temperature and film thickness for various parameters are examined in detail.

Figure 1 exemplifies the film thickness profiles for various zeta potentials and shows that film thickness increases with increase in zeta potential; this shows the effect of EDL on film thickness; also the effect of EDL on pressure is not so significant. For, the isothermal and thermal pressure distributions for load $W = 1.3674E-05$, speed $U = 1.0218E-12$ with zeta potential $\xi = 100mv$ is illustrated in Figure 2. It is observed that, the pressure spike is noticeable in thermal case but not in isothermal case. Isothermal and thermal film thickness distributions for $W = 1.3674E-05$, $U = 1.0218E-12$ with $\xi = 100mv$ is demonstrated in Figure 3, and isothermal minimum film thickness has a higher value as compared to thermal minimum film thickness. Figure4 demonstrates the temperature profiles for $W = 1.3674E-05$, $U = 1.0218E-12$ with $\xi = 100mv$ as usual the middle layer temperature is higher than the surface temperature distributions.

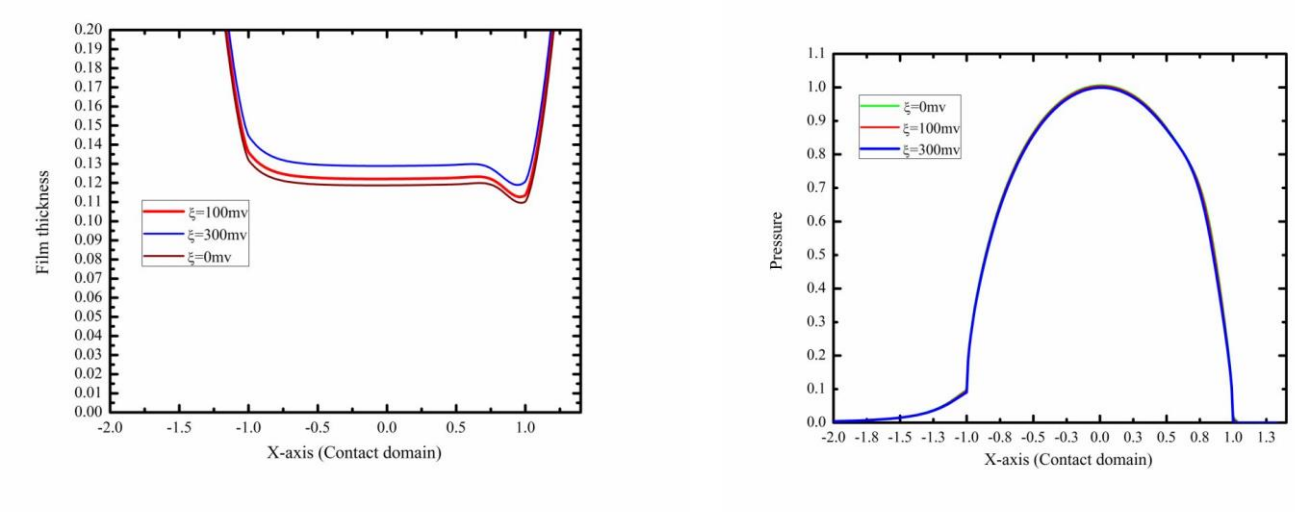

Figure 1. Film thickness and pressure distributions for the load $W = 1.3674E-05$, *speed* $U = 1.0218E-12$ *with different zeta potentials.*

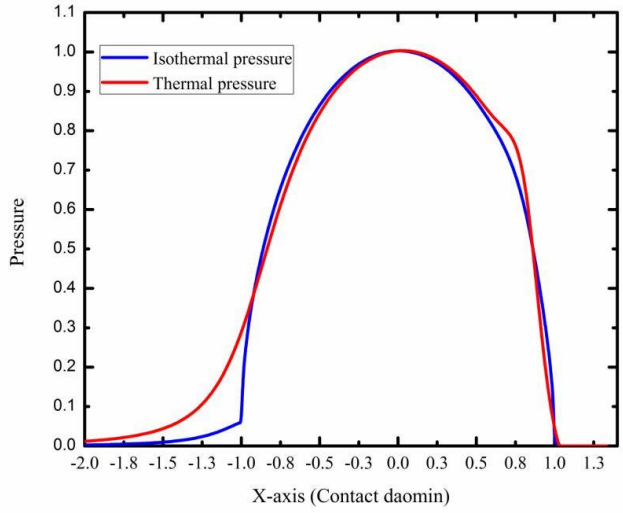

Figure 2. Isothermal and thermal pressure profiles for $W = 1.3674E-05, U = 1.0218E-12$ *with zeta potential* $\xi = 100mv$.

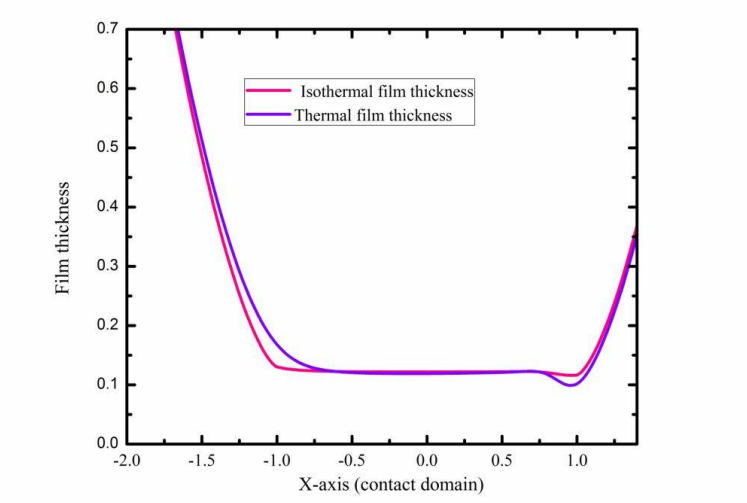

Figure 3. Isothermal and thermal film thickness profiles for $W = 1.3674E-05$, $U = 1.0218E-12$ *and zeta potential* $\xi = 100mv$.

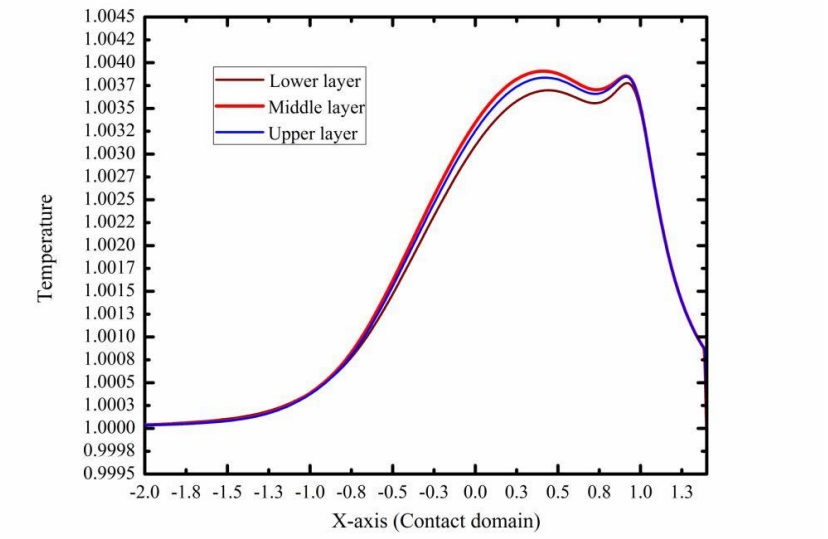

Figure 4. Temperature profiles for $W = 1.3674E-05$, $U = 1.0218E-12$ *with* $\xi = 100mv$.

Figure 5 describes the apparent viscosity profiles for isothermal and thermal cases by considering the operating parameters $W = 1.3674E-05$, $U = 1.0218E-12$ with $\xi = 0$ and $\xi = 100mv$. In view of increased apparent viscosity is due to the effect of EDL. While temperature effect is taken into account the apparent viscosity decreases. This shows the leverage of temperature interpretation on electro-viscous effect which is significant and it should be deliberated while analyzing the EDL effect on EHL. The study of Dowson and Higginson [55] reveals that, as load increases, the pressure spike and film thickness decreases, in contrast to load variation, pressure spike and film thickness increases with increase in speed and these findings are demonstrated in Figures 6-9. Associating Figures 3 and 6, film thickness profiles moves downwards as load increases. The effect of temperature on fluid film thickness for various speed is illustrated in Figures. 8 and 9 at constant load and zeta potential, it depicts that isothermal as well as thermal film thickness increases as the speed increases. The isothermal film thickness is much thicker than the thermal film thickness, as can be seen in Figures 8 and 9. This is due to the increase in temperature in the contact area, which reduces the effect of the EDL on the film thickness.

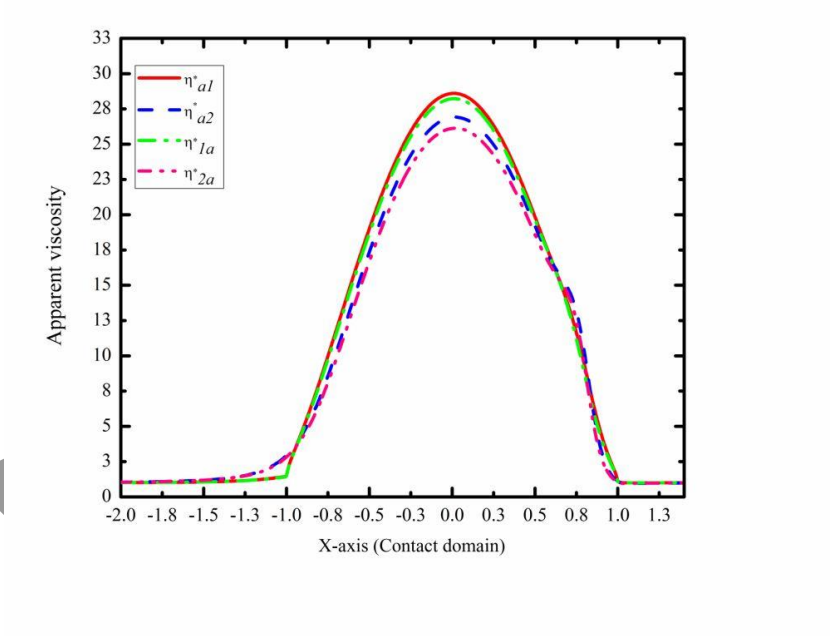

Figure 5. Apparent viscosity profiles for different cases, η_{a1}^{*} is isothermal apparent viscosity with the effect of EDL, η_{a2}^{*} is the thermal apparent viscosity with EDL effect η_{1a}^{*} is the isothermal apparent viscosity without EDL effect and η_{2a}^{*} is thermal apparent viscosity distribution without considering the EDL effect.

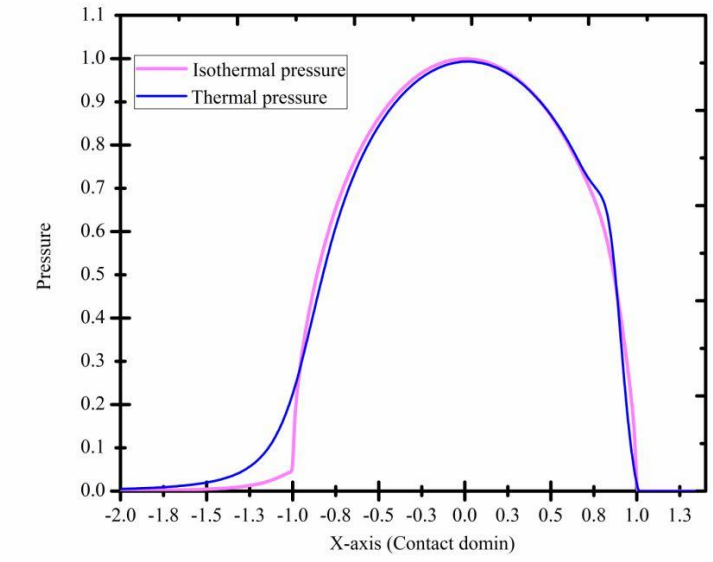

Figure 6. Pressure distributions for $W = 2.2140E-05, U = 1.0218E-12$ with $\xi = 100mv$.

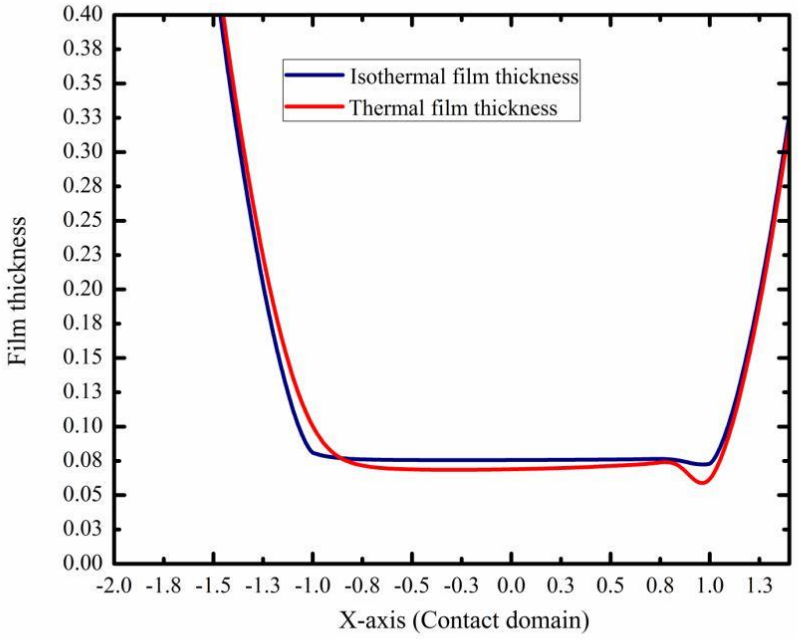

Figure 7. Isothermal and thermal film thickness distributions for $W = 2.2140E-05$, $U = 1.0218E-12$ *with* $\xi = 100mv$.

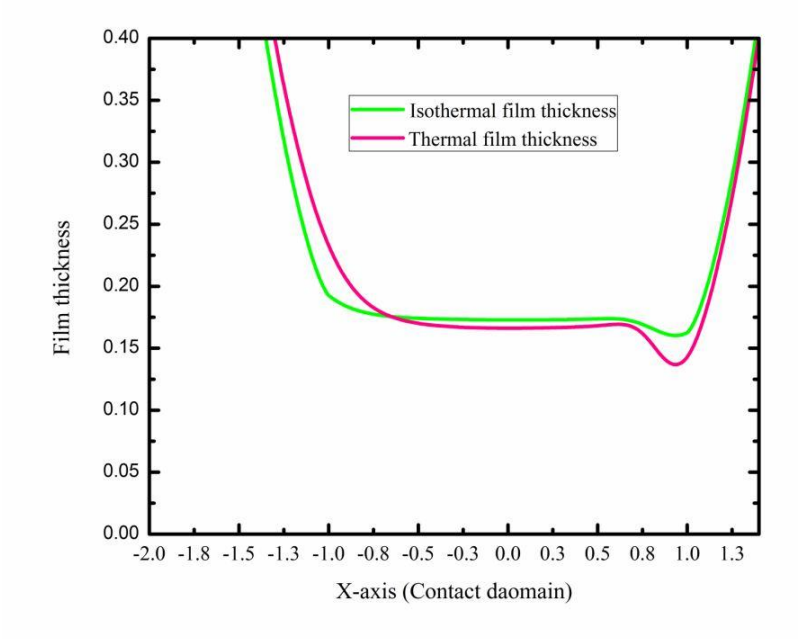

Figure 8. Fluid film thickness profiles for $U = 1.7031E-12$ $W = 1.3674E-05$ *with* $\xi = 100mv$.

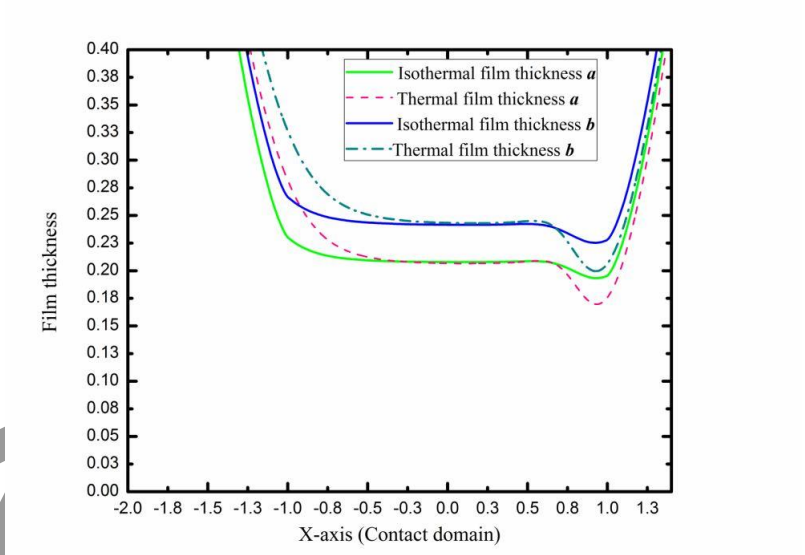

Figure 9. Isothermal and thermal film thickness profiles for various speed viz., a)$U = 2.3843E-12$, and b)$U = 3.0655E-12$ *at a constant* $W = 1.3674E-05$ *and* $\xi = 100mv$

The pressure profiles for different speeds are shown in Figures 10 and 11. It can be seen that the pressure peak increases with increasing velocity. When comparing isothermal and thermal pressure profiles, it is clear that the isothermal pressure peak is lower than the thermal pressure peak. This phenomenon is due to the effect of the EDL, which is more pronounced in the isothermal case; in the thermal case, the effect of the EDL is reduced due to the reduction in apparent viscosity. Figures 12 and 13 show the temperature profiles for different velocities at constant load and constant zeta potential.

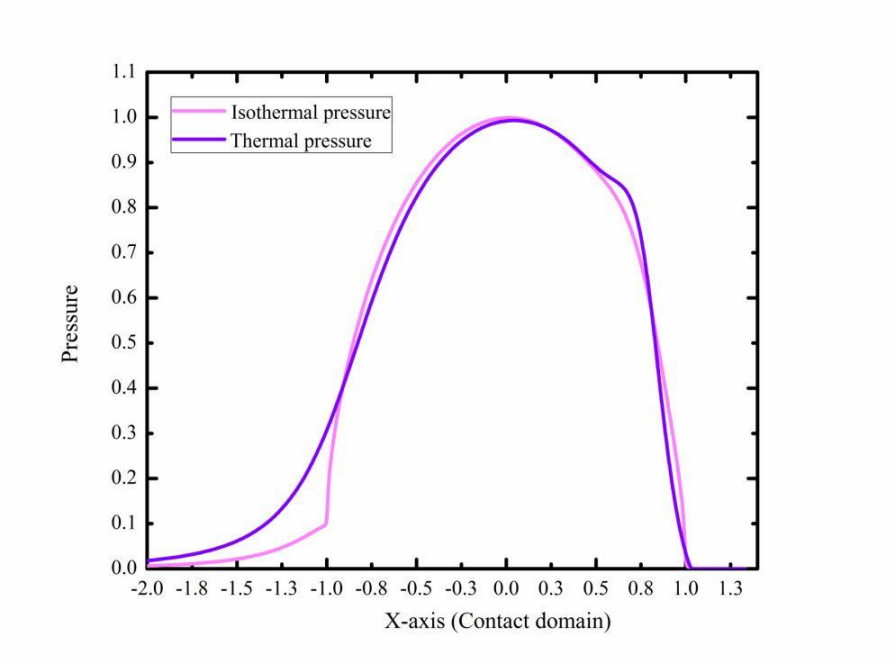

Figure 10. Pressure profiles for $W = 1.3674E-05$, $U = 1.7031E-12$ *with* $\xi = 100mv$.

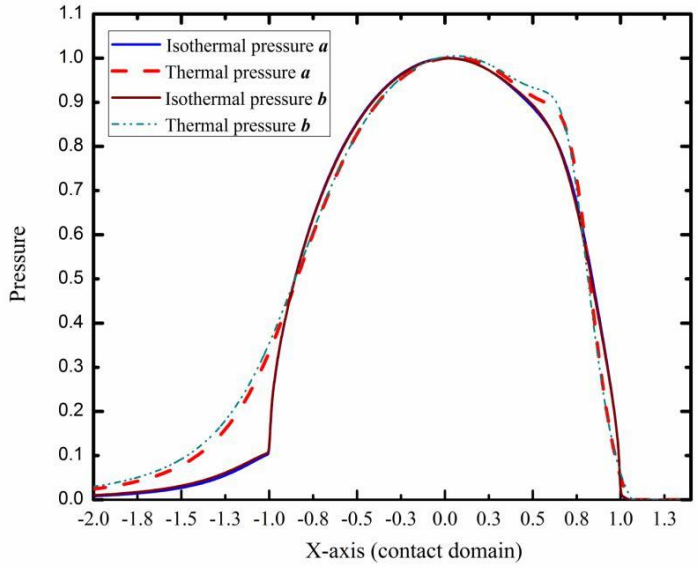

Figure 11. Isothermal and thermal pressure distributions for a) $U = 2.3843E-12$ *and b)* $U = 3.0655E-12$ *at the constant* $W = 1.3674E-05$ *and* $\xi = 100mv$.

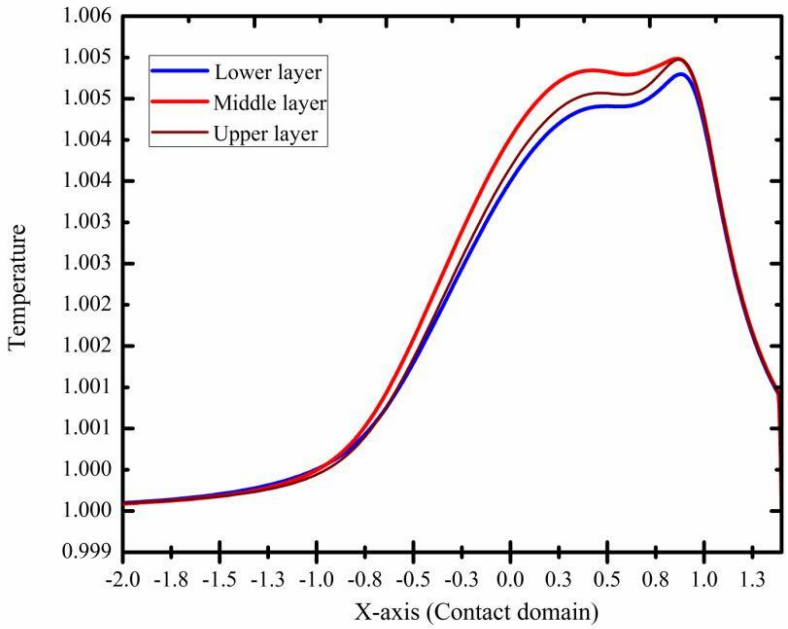

Figure 12. Temperature profiles for $W = 1.3674E-05$ *and* $\xi = 100mv$ *with speed* $U = 1.7031E-12$

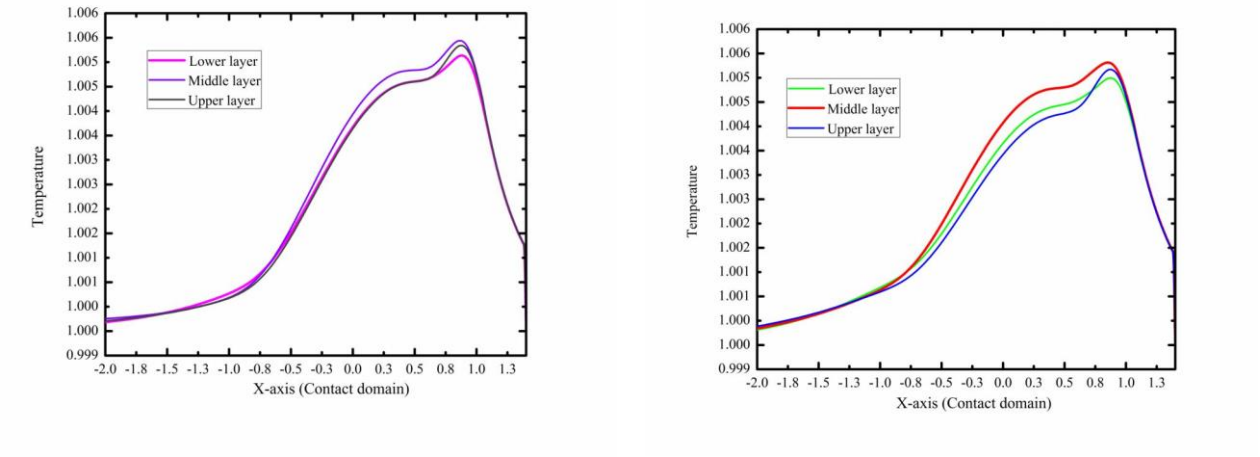

(A) ***(B)***

Figure 13. A and B Temperatures profiles for different speed $U = 2.3843E-12$ *and* $U = 3.0655E-12$ *respectively; at a constant load* $W = 1.3674E-05$ *and zeta potential* $\xi = 100mv$.

Table 1. shows the material parameters used in the present investigation. The comparisons of minimum and central film thickness for isothermal and thermal cases are given. Minimum film thickness for isothermal case is always larger than that of minimum film thickness of thermal case which is given in Table 2.

Table 1. The material parameters used in the present study.

Properties of lubricant and contacting material surfaces	
Thermal conductivity of water(W/m K)	0.58
Thermal conductivity of steel(W/m K)	46
Thermal conductivity of SiO_2(W/m K)	0.04
Specific heat of Water (J/Kg ^oC)	4200
Specific heat of steel (J/Kg ^oC)	470
Specific heat of SiO_2 (J/Kg ^oC)	670
Density of water (Kg/m^3)	1000
Density of steel (Kg/m^3)	7850
Density of SiO_2 (Kg/m^3)	2700

Table 2. Comparison of minimum and central film thickness for isothermal and thermal cases at different load and speed

Sl. No.	Load WE-05	Speed UE-12	Isothermal film thickness H_{min}	H_{cen}	Thermal film thickness $H_{min.}$	$H_{cen.}$
1	1.3674	1.0218	0.1161	0.1220	0.0990	0.1190
2	2.2140		0.0724	0.0757	0.0588	0.0689
3	0.68122		0.2573	0.2807	0.2150	0.2649
4	1.3674	1.7031	0.1603	0.1729	0.1368	0.1662
5		2.3843	0.1932	0.2078	0.1696	0.2066
6		3.0655	0.2252	0.2433	0.1996	0.2343

4 Conclusion

In the present study, we consider the EDL effect on the problem of thermal line contact EHL. The mathematical model of the physical problem is solved using the Krylov subspace method and the following conclusions have been drawn from the above study, The effect of EDL depends mainly on the zeta potential. As the zeta potential increases, fluid film also increases. The thermal minimum film thickness is lower than the isothermal minimum film thickness due to the temperature increase, which reduces the effect of EDL on the film thickness. The effect of EDL on film thickness is significant, but not as significant on pressure, since equation (4) shows that electroviscosity is proportional to the square of the zeta potential or inversely proportional to the quartic of the film thickness. Therefore, the influence of EDL is significant for a very thin lubrication film, but decreases rapidly as the film thickness increases In the future, this work can be extended to the point contact EDL problem by considering the effects of surface roughness, temperature and slider to roller ratio on fluid film and pressure.

References

[1] S. Wen and P. Huang, *Principles of tribology*, 3rd ed. TsingHua University Press, Beijing, 2008.

[2] D. C. PRIEVE and S. G. BIKE, "Electrokinetic repulsion between two charged bodies undergoing sliding motion," *Chem. Eng. Commun.*, vol. 55, no. 1–6, pp. 149–164, 1987.

[3] S. G. Bike and D. C. Prieve, "Electrohydrodynamic lubrication with thin double layers," *J. Colloid Interface Sci.*, vol. 136, no. 1, pp. 95–112, 1990.

[4] J. Luo, S. Wen, and P. Huang, "Thin film lubrication. Part I. Study on the transition between EHL and thin film lubrication using a relativeoptical interference intensity technique," *Wear*, vol. 194, no. 1–2, pp. 107–115, 1996.

[5] B. Zhang and N. Umehara, "Hydrodynamic lubrication theory considering electric double layer for very thin water film lubrication ofceramics," *JSME Int. J. Ser. C Mech. Syst. Mach. Elem. Manuf.*, vol. 41, no. 2, pp. 285–290, 1998.

[6] D. Li, "Electro-viscous effects on pressure-driven liquid flow in microchannels," *Colloids surfaces A Physicochem. Eng. Asp.*, vol. 195, no. 1–3, pp. 35–57, 2001.

[7] L. Ren, D. Li, and W. Qu, "Electro-viscous effects on liquid flow in microchannels," *J. Colloid Interface Sci.*, vol. 233, no. 1, pp. 12–22, 2001.

[8] L. Ren, W. Qu, and D. Li, "Interfacial electrokinetic effects on liquid flow in microchannels," *Int. J. Heat Mass Transf.*, vol. 44, no. 16, pp. 3125–3134, 2001.

[9] P. Huang, P. L. Wong, Y. Meng, and S. Wen, "Influences of electric double layer on the thin lubrication film thickness and pressure," *Jixie Gongcheng Xuebao/Chinese J. Mech. Eng.*, vol. 38, no. 8, pp. 9–13, 2002.

[10] P. L. Wong, P. Huang, and Y. Meng, "The effect of the electric double layer on a very thin water lubricating film," *Tribol. Lett.*, vol. 14, pp. 197–203, 2003.

[11] W.-L. Li, "Effects of electrodouble layer (EDL) and surface roughness on lubrication theory," *Tribol. Lett.*, vol. 20, pp. 53–61, 2005.

[12] S. Bai, P. Huang, Y. Meng, and S. Wen, "Modeling and analysis of interfacial electro-kinetic effects on thin film lubrication," *Tribol. Int.*, vol. 39, no. 11, pp. 1405–1412, 2006.

[13] B. Shaoxian and H. Ping, "Experimental and numerical study on influence of electro-viscosity of electric double layer in thin filmlubrication," *Chinese J. Mech. Eng.*, vol. 40, no. 5, pp. 34–38, 2004.

[14] X. Wang, S. Bai, and P. Huang, "Theoretical analysis and experimental study on the influence of electric double layer on thin filmlubrication," *Front. Mech. Eng. China*, vol. 1, pp. 370–373, 2006.

[15] S. X. Bai, *Theoretical and experimental study on influence of electric double layer on thin film lubrication*. Ph.D. South China University of Technology, Guangzhou , 2007.

[16] S. Z. Wen, *Interface Science and Technology*. TsingHua University Press, Beijing, 2011.

[17] Y. Chen, Q. Zuo, and P. Huang, "Influence of electric double layers on elastohydrodynamic lubricating water film in line contact," *Proc. Inst. Mech. Eng. Part N J. Nanoeng. Nanosyst.*, vol. 227, no. 4, pp. 196–198, 2013.

[18] V. B. Awati, P. Obannavar, and M. Kumar, "Newton-GMRES-Method for the Scritinization of

electric double layer and surface roughness on EHL line contactproblem," *J. Mech. Eng. Sci.*, pp. 9370–9382, 2023.
[19] H. S. Cheng and B. Sternlicht, "A Numerical Solution for the Pressure, Temperature, and Film Thickness Between Two Infinitely Long,Lubricated Rolling and Sliding Cylinders, Under Heavy Loads," *J. Basic Eng.*, vol. 87, no. 3, pp. 695–704, 1965, doi: 10.1115/1.3650647.
[20] M. K. Ghosh and B. J. Hamrock, "Thermal elastohydrodynamic lubrication of line contacts," *ASLE Trans.*, vol. 28, no. 2, pp. 159–171, 1985.
[21] F. Sadeghi and P. C. Sui, "Thermal Elastohydrodynamic Lubrication of Rolling/Sliding Contacts," *J. Tribol.*, vol. 112, no. 2, pp. 189–195, 1990, doi: 10.1115/1.2920241.
[22] H. Salehizadeh and N. Saka, "Thermal Non-Newtonian Elastohydrodynamic Lubrication of Rolling Line Contacts," *J. Tribol.*, vol. 113, no. 3, pp. 481–491, 1991, doi: 10.1115/1.2920649.
[23] R. Wolff, T. Nonaka, A. Kubo, and K. Matsuo, "Thermal Elastohydrodynamic Lubrication of Rolling/Sliding Line Contacts," *J. Tribol.*, vol. 114, no. 4, pp. 706–713, 1992, doi: 10.1115/1.2920939.
[24] R. Wolff and A. Kubo, "The Application of Newton-Raphson Method to Thermal Elastohydrodynamic Lubrication of Line Contacts," *J. Tribol.*, vol. 116, no. 4, pp. 733–740, 1994, doi: 10.1115/1.2927327.
[25] X. Liu and P. Yang, "Analysis of the thermal elastohydrodynamic lubrication of a finite line contact," *Tribol. Int.*, vol. 35, no. 3, pp. 137–144, 2002.
[26] P. Yang, J. Wang, and M. Kaneta, "Thermal and Non-Newtonian Numerical Analyses for Starved EHL Line Contacts," *J. Tribol.*, vol. 128, no. 2, pp. 282–290, 2005, doi: 10.1115/1.2164465.
[27] W. Habchi, D. Eyheramendy, S. Bair, P. Vergne, and G. Morales-Espejel, "Thermal elastohydrodynamic lubrication of point contacts using a Newtonian/generalized Newtonian lubricant," *Tribol. Lett.*, vol. 30, pp. 41–52, 2008.
[28] M. Carli, K. J. Sharif, E. Ciulli, H. P. Evans, and R. W. Snidle, "Thermal point contact EHL analysis of rolling/sliding contacts with experimental comparison showing anomalous film shapes," *Tribol. Int.*, vol. 42, no. 4, pp. 517–525, 2009.
[29] Q. Zuo, T. Lai, and P. Huang, "The effect of the electric double layer on very thin thermal elastohydrodynamic lubricating film," *Tribol. Lett.*, vol. 45, pp. 455–463, 2012.
[30] X.-L. Yan, X.-L. Wang, and Y.-Y. Zhang, "A numerical study of fatigue life in non-Newtonian thermal EHL rolling–sliding contacts with spinning," *Tribol. Int.*, vol. 80, pp. 156–165, 2014.
[31] B. Zhang, J. Wang, M. Omasta, and M. Kaneta, "Effect of fluid rheology on the thermal EHL under ZEV in line contact," *Tribol. Int.*, vol. 87, pp. 40–49, 2015.
[32] H. C. Liu, B. B. Zhang, N. Bader, G. Poll, and C. H. Venner, "Influences of solid and lubricant thermal conductivity on traction in an EHL circular contact," *Tribol. Int.*, vol. 146, p. 106059, 2020, doi: https://doi.org/10.1016/j.triboint.2019.106059.
[33] X. Meng, J. Wang, H. Nishikawa, and G. Nagayama, "Effects of boundary slips on thermal elastohydrodynamic lubrication under pure rolling and opposite sliding contacts," *Tribol. Int.*, vol. 155, p. 106801, 2021, doi: https://doi.org/10.1016/j.triboint.2020.106801.
[34] K. Ono, "Modified Reynolds equations for thin film lubrication analysis with high viscosity surface layers on both solid surfaces and analysis of micro-tapered bearing," *Tribol. Int.*, vol. 151, p. 106515, 2020, doi: https://doi.org/10.1016/j.triboint.2020.106515.
[35] V. B. Awati, M. Kumar N, and N. M. Bujurke, "Numerical solution of thermal EHL line contact with bio-based oil as lubricant," *Aust. J. Mech. Eng.*, vol. 20, no. 1, pp. 231–244, 2022.
[36] M. Tošić, R. Larsson, and T. Lohner, "Thermal Effects in Slender EHL Contacts," *Lubricants*, vol. 10, no. 5, 2022, doi: 10.3390/lubricants10050089.
[37] C. Fang, Y. Peng, W. Zhou, and X. Meng, "A fully coupled finite element solution for the mixed elastohydrodynamic lubrication of finite line contacts," *Tribol. Int.*, vol. 194, p. 109530, 2024, doi: https://doi.org/10.1016/j.triboint.2024.109530.
[38] G. Yu, Y. Zhao, Z. Fu, and Z. Chen, "Application of back propagation neural network in the analysis of isothermal elastohydrodynamic lubrication," *Tribol. Int.*, vol. 198, p. 109883, 2024, doi: https://doi.org/10.1016/j.triboint.2024.109883.
[39] Y. Zhao and P. L. Wong, "Thermal-EHL analysis of slip/no-slip contact at high slide-to-roll ratio," *Tribol. Int.*, vol. 153, p. 106617, 2021.

[40] R. Hjelm and J. Wahlström, "Influence of Manufacturing Error Tolerances on Thermal EHL Behavior of Gears," *Lubricants*, vol. 10, no. 11, p. 323, 2022.
[41] Y. Saad, *Iterative methods for sparse linear systems*. SIAM, 2003.
[42] E. Stiefel, "Methods of conjugate gradients for solving linear systems," *J. Res. Nat. Bur. Stand.*, vol. 49, pp. 409–435, 1952.
[43] J. K. Reid, "On the method of conjugate gradients for the solution of large sparse systems of linear equations," in *Proc. Conf. on Large Sparse Set of Linear Equations, 1971*, 1971.
[44] G. H. Golub and D. P. O'Leary, "Some history of the conjugate gradient and Lanczos algorithms: 1948–1976," *SIAM Rev.*, vol. 31, no. 1, pp. 50–102, 1989.
[45] A. Greenbaum, *Iterative methods for solving linear systems*. SIAM, 1997.
[46] Y. Saad and M. H. Schultz, "GMRES: A generalized minimal residual algorithm for solving nonsymmetric linear systems," *SIAM J. Sci. Stat. Comput.*, vol. 7, no. 3, pp. 856–869, 1986.
[47] Y. Saad and H. A. Van Der Vorst, "Iterative solution of linear systems in the 20th century," *J. Comput. Appl. Math.*, vol. 123, no. 1–2, pp. 1–33, 2000.
[48] R. W. Freund, G. H. Golub, and N. M. Nachtigal, "Iterative solution of linear systems," *Acta Numer.*, vol. 1, pp. 57–100, 1992.
[49] V. Simoncini and D. B. Szyld, "Recent computational developments in Krylov subspace methods for linear systems," *Numer. Linear Algebr. with Appl.*, vol. 14, no. 1, pp. 1–59, 2007.
[50] K. Chen, "Discrete wavelet transforms accelerated sparse preconditioners for dense boundary element systems," *Electron. Trans. Numer. Anal.*, vol. 8, pp. 138–153, 1999.
[51] I. Daubechies, *Ten lectures on wavelets*. SIAM, 1992.
[52] J. Ford, K. Chen, and L. Scales, "A new wavelet transform preconditioner for iterative solution of elastohydrodynamic lubrication problems," *Int. J. Comput. Math.*, vol. 75, no. 4, pp. 497–513, 2000.
[53] S. Z. Wen and P. R. Yang, *Elastohydrodynamic Lubrication*. TsingHua University Press, Beijing, 1992.
[54] C. J. A. Roelands, W. O. Winer, and W. A. Wright, "Correlational aspects of the viscosity-temperature-pressure relationship of lubricating oils (Dr In dissertation at Technical University of Delft, 1966)," 1971.
[55] D. Dowson, "Elastohydrodynamic Lubrication/Dowson D," *Higginson GR-Oxford Pergamon Press Ltd*, 1977.
[56] J. Liesen and Z. Strakos, *Krylov subspace methods: principles and analysis*. Numerical Mathematics and Scie, 2013.